

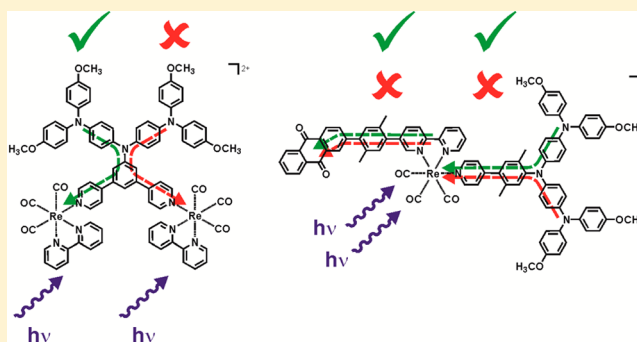
Photoinduced Electron Transfer in Rhenium(I)–Oligotriarylamine Molecules

Annabell G. Bonn, Markus Neuburger, and Oliver S. Wenger*

Department of Chemistry, University of Basel, St. Johannis-Ring 19, CH-4056 Basel, Switzerland

Supporting Information

ABSTRACT: Two molecular triads with an oligotriarylamine multielectron donor were synthesized and investigated with a view to obtaining charge-separated states in which the oligotriarylamine is oxidized 2-fold. Such photoinduced accumulation of multiple redox equivalents is of interest for artificial photosynthesis. The first triad was comprised of the oligotriarylamine and two rhenium(I) tricarbonyl diimine photosensitizers each of which can potentially accept one electron. In the second triad the oligotriarylamine was connected to anthraquinone, in principle an acceptor of two electrons, via a rhenium(I) tricarbonyl diimine unit. With nanosecond transient absorption spectroscopy (using an ordinary pump–probe technique) no evidence for the generation of 2-fold oxidized oligotriarylamine or 2-fold reduced anthraquinone was found. The key factors limiting the photochemistry of the new triads to simple charge separation of one electron and one hole are discussed, and the insights gained from this study are useful for further research in the area of charge accumulation in purely molecular (nanoparticle-free) systems. An important problem of the rhenium-based systems considered here is the short wavelength required for photoexcitation. In the second triad, photogenerated anthraquinone monoanion is protonated by organic acids, and the resulting semiquinone species leads to an increase in lifetime of the charge-separated state by about an order of magnitude. This shows that the proton-coupled electron transfer chemistry of quinones could be beneficial for photoinduced charge accumulation.



INTRODUCTION

Donor–photosensitizer–acceptor molecules have been very frequently employed for driving-force or distance-dependence studies of (photoinduced) electron transfer.¹ Many important insights regarding the so-called Marcus inverted region and the mechanisms of long-range electron transfer were gained by such investigations.² In numerous cases relatively long-lived electron–hole pairs were observed after excitation with visible light, and the primary charge-separation events in bacterial photosynthetic reaction centers were successfully mimicked.³ However, as long as single electrons are separated from single holes, it is difficult to perform much useful secondary chemistry with photogenerated charge-separated states, because many of the most interesting fuel-forming reactions require multiple redox equivalents.⁴ Light-driven separation of multiple electrons from multiple holes remains a significant challenge. Nanoparticles can readily accommodate multiple charges,⁵ but in purely molecular systems the accumulation of several electrons or holes is more difficult, and there are relatively few experimental studies that have focused on this particular aspect of photoinduced electron transfer in donor–sensitizer–acceptor molecules.⁶

Oligotriarylamine (OTAs) can release multiple electrons at decent electrochemical potentials, and their one- and two-electron oxidized forms often have characteristic spectroscopic

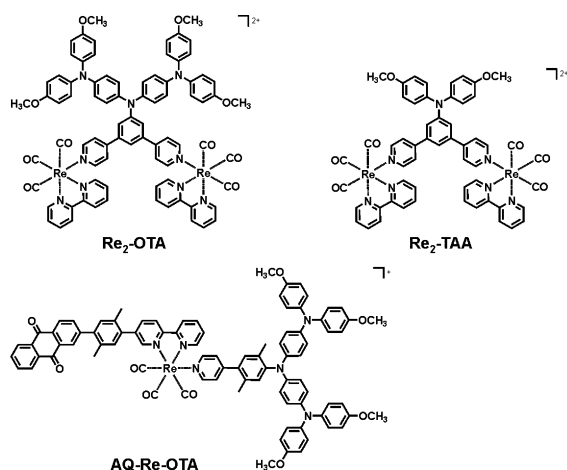
signatures, which should be distinguishable from one another by transient absorption spectroscopy.⁷ Indeed, a recent study of OTA–Ru(2,2′-bipyridine)₃²⁺–TiO₂ systems was able to provide evidence for the 2-fold oxidation of an OTA molecule after a two-photon excitation process.^{5c} In our work, we synthesized a molecule in which an OTA unit is covalently connected to two rhenium(I) tricarbonyl diimine photosensitizers (Re₂–OTA, Scheme 1). We aimed to explore whether through simultaneous excitation of the two photosensitizers it would be possible to access a (presumably short-lived) charge-separated state in which the OTA unit is oxidized twice, while each of the rhenium complexes would be in its one-electron reduced form. A reference molecule with a simple triarylamine (TAA) one-electron donor was also investigated (Re₂–TAA, Scheme 1).

Quinones are two-electron acceptors, and the uptake of the second electron occurs with particular ease in the presence of hydrogen-bond donors or Brønsted acids.⁸ 9,10-anthraquinone (AQ) produces relatively clear spectroscopic signatures in its reduced forms, which are readily detectable by transient absorption spectroscopy.^{8b,9} Therefore, we decided to synthesize a triad comprised of an OTA donor, a single rhenium(I)

Received: July 8, 2014

Published: October 1, 2014

Scheme 1. Chemical Structures of the Key Compounds Investigated in This Study



photosensitizer, and an AQ acceptor (OTA–Re–AQ, Scheme 1). The purpose was to explore whether through 2-fold (consecutive) photoexcitation of the same rhenium(I) sensitizer a charge-separated state containing OTA^{2+} and AQ^{2-} (or protonated forms thereof) could be accessible.

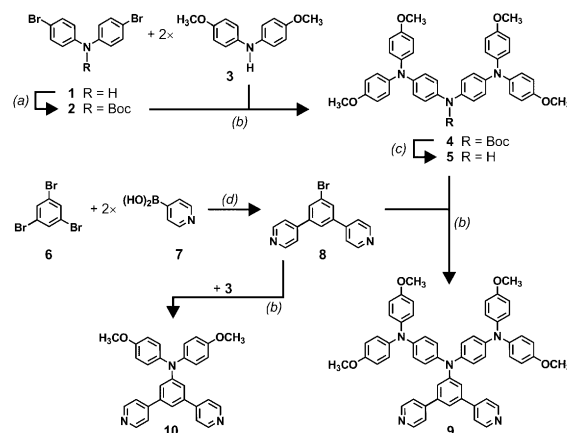
Rhenium(I) tricarbonyl diimine sensitizers are popular choices for studies of photoinduced electron (and energy) transfer,¹⁰ and we used them because their molecular structure offered some advantages for the synthesis of our target molecules. The *p*-xylene linkers ensure a suitable balance between conformational dynamics facilitating electron transfer and good solubility.¹¹

We were not able to detect any 2-fold oxidized OTA or 2-fold reduced AQ in either of the systems from Scheme 1 but gained some valuable insights, which we consider useful for future research in the area of generating two-electron oxidized or two-electron reduced photoproducts in purely molecular systems. In addition, our study provides insight into the influence of acids of different strengths on the accessible photoproducts (and their lifetimes) in systems with quinone acceptors. The proton-coupled electron transfer (PCET) chemistry of quinones could indeed prove to be useful for the accumulation of multiple electrons on such units.

RESULTS AND DISCUSSION

Synthesis and Crystallographic Studies. The triarylamine- and oligotriarylamine-decorated ligands of the Re_2 -TAA and Re_2 -OTA complexes were synthesized following the strategy outlined in Scheme 2. The starting point was commercial bis(4-bromophenyl)amine (**1**), which was protected with a Boc group (**2**) prior to performing Buchwald–Hartwig coupling with dianisylamine (**3**).^{7c} The coupling product (**4**) was deprotected,¹² and the resulting secondary amine (**5**) was reacted with compound **8**, which in turn was synthesized from 1,3,5-tribromobenzene (**6**) and pyridine-4-boronic acid hydrate (**7**). Compounds **5** and **8** were isolated in pure forms with yields of 84% and 36%, respectively, and the final coupling reaction to afford ligand **9** proceeded with a yield of 71%. Ligand **10** was obtained in 83% yield via Pd-catalyzed N–C coupling between dianisylamine (**3**) and compound **8**. Coordination of ligands **9** and **10** to the final rhenium(I) complexes was accomplished using the $[\text{Re}(\text{bpy})(\text{CO})_3(\text{OTf})]$ precursor (bpy = 2,2'-bipyridine, OTf = triflate).¹³ The yields

Scheme 2. Synthetic Strategies Leading to the Amino-Decorated Pyridine Ligands Required for the Re_2 -OTA and Re_2 -TAA Molecules^a

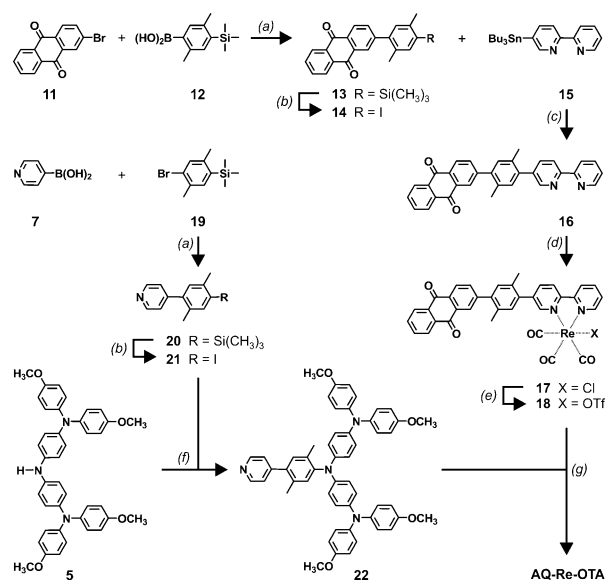


^a(a) 4-(*N,N*-Dimethylamino)pyridine, di-*tert*-butyl dicarbonate, THF, reflux, 3 h. (b) ^tBuONa, Pd(dba)₂, (HP^tBu₃)BF₄, toluene, reflux. (c) CF₃COOH, acetone, 20 °C; (d) Pd(PPh₃)₄, THF/H₂O, Na₂CO₃, reflux, 24 h.

of isolated pure Re_2 -OTA and Re_2 -TAA were 37% and 50%, respectively.

The synthetic pathway leading to the AQ–Re–OTA triad is shown in Scheme 3. 2-Bromo-9,10-anthraquinone (**11**) was

Scheme 3. Synthetic Strategy Leading to the AQ–Re–OTA Triad^a



^a(a) Pd(PPh₃)₄, toluene/EtOH/H₂O, Na₂CO₃, reflux. (b) ICl, CH₂Cl₂/CH₃CN, 0 °C. (c) Pd(PPh₃)₄, *m*-xylene, reflux, 70 h. (d) Re(CO)₅Cl, toluene, reflux. (e) CF₃SO₃H, CH₂Cl₂, Et₂O, 20 °C. (f) ^tBuOK, Pd(dba)₂, (HP^tBu₃)BF₄, toluene, 100 °C. (g) CH₃OH, CHCl₃, reflux, 43 h.

coupled to 4-trimethylsilyl-2,5-dimethylphenylboronic acid (**12**)¹⁴ using the Pd(PPh₃)₄ catalyst. The coupling product (**13**) was deprotected with ICl, and the resulting iodo compound (**14**) was coupled to 5-(tri(*n*-butyl)stannyl)-2,2'-bipyridine (**15**)¹⁵ to afford the final anthraquinone-equipped bpy ligand (**16**) in 73% global yield. For this part of the

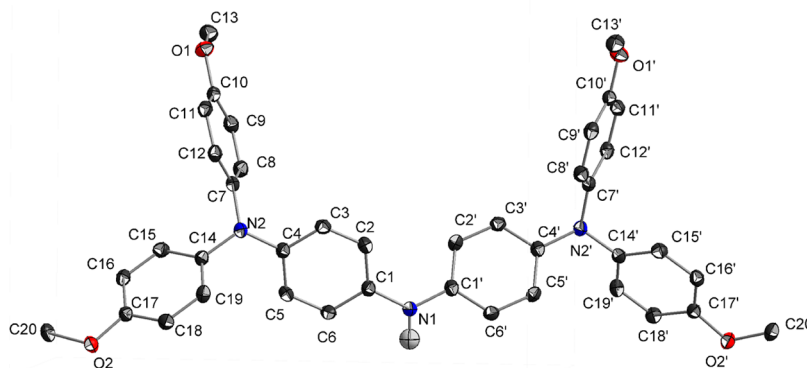


Figure 1. Crystallographic structure of oligotriarylamine **5**. Anisotropic displacement parameters are drawn at the 50% probability level.

synthesis we followed our own previously published strategy.¹⁶ Coordination to rhenium(I) occurred by reacting ligand **16** with pentacarbonylchlororhenium(I), followed by exchanging the chloro ligand of complex **17** by a very weakly coordinating triflate (**18**). The OTA-decorated pyridine ligand (**22**) was obtained by reacting pyridine-4-boronic acid hydrate (**7**) with 1-bromo-4-trimethylsilyl-2,5-dimethylbenzene (**19**), followed by deprotection of the trimethylsilyl group of the coupling product (**20**) with ICl. The resulting iodo compound (**21**) was coupled to oligotriarylamine **5** to afford ligand **22**, which was reacted with complex **18** to give AQ-Re-OTA in 47% yield.

All key compounds were characterized by ¹H NMR spectroscopy, high-resolution ESI mass spectrometry, and CHN elemental analysis. Their NMR and mass spectra are shown in the Supporting Information, and detailed synthetic procedures and product characterization data for all new compounds appearing in Schemes 1–3 can be found in the Experimental Section.

Single crystals of oligotriarylamine **5** were obtained by slow evaporation of an acetone solution. The result of an X-ray diffraction study is shown in Figure 1, and crystallographic details are in the Supporting Information. The key observation in Figure 1 is the propeller-shaped structure of all triarylamino units, which is a common feature of this class of compounds and which is responsible for their relatively low basicity, an aspect that will become important in the optical spectroscopic studies presented below.

Optical Spectroscopy and Electrochemistry. In Figure 2a the optical absorption spectra of the three compounds from Scheme 1 in CH₃CN are shown. Compared to the [Re(bpy)-

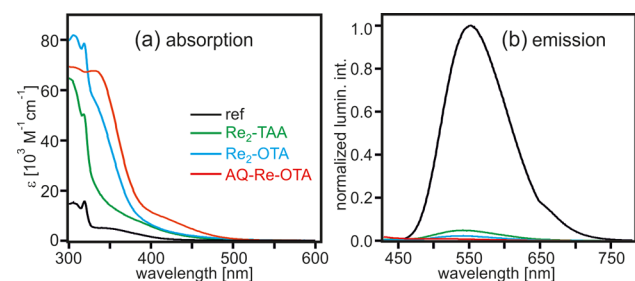


Figure 2. (a) Optical absorption spectra of the three compounds from Scheme 1 and [Re(bpy)(CO)₃(py)]⁺ (ref) in CH₃CN. (b) Normalized luminescence spectra of the same four compounds in deoxygenated CH₃CN obtained after excitation at 350 nm. The relative intensities of the individual luminescence spectra were corrected for differences in absorbance at the excitation wavelength.

(CO)₃(py)]⁺ (py = pyridine) reference complex (ref, black trace) the molecules from Scheme 1 have a significantly higher molar extinction coefficient, which is presumably an effect of increased π -conjugation.^{11b,17} The luminescence emitted by Re₂-OTA, Re₂-TAA, and AQ-Re-OTA in CH₃CN following excitation at 350 nm is significantly weaker than that of [Re(bpy)(CO)₃(py)]⁺ (Figure 2b), and this is due to excited-state quenching by intramolecular electron transfer as demonstrated below.

Cyclic voltammograms of [Re(bpy)(CO)₃(py)]⁺, Re₂-TAA, Re₂-OTA, and AQ-Re-OTA measured in CH₃CN with 0.1 M TBAPF₆ are shown in Figure 3. Some of the voltammograms

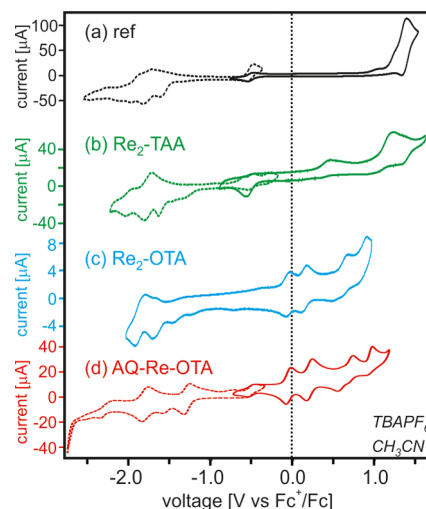


Figure 3. Cyclic voltammograms of the [Re(bpy)(CO)₃(py)]⁺ reference complex (ref) and the three compounds from Scheme 1 in dry CH₃CN with 0.1 M TBAPF₆. The voltage sweep rate was 0.1 V/s; the waves at −0.51 V are due to decamethylferrocene, which was added in small quantities for internal voltage calibration. (a, b, and d) Oxidative (solid lines) and reductive (dashed lines) sweeps were performed separately because this gave higher quality results than scans over the entire −2.7 to 1.7 V vs Fc⁺/Fc range.

were recorded in two separate voltage sweeps, one extending from −0.8 V vs Fc⁺/Fc to positive potentials (solid lines) and another one between −0.4 V vs Fc⁺/Fc and more negative potentials (dashed lines) because this gave higher quality results. The waves at −0.51 V are due to decamethylferrocene, which was added in small quantities for internal voltage calibration.¹⁸

Table 1. Reduction Potentials (in volts vs Fc^+/Fc) for the Various Electrochemically Active Components of Re_2 -TAA, Re_2 -OTA, AQ-Re-OTA, and $[\text{Re}(\text{bpy})(\text{CO})_3(\text{py})]\text{OTf}$ (ref) in CH_3CN as Determined from the Cyclic Voltammetry Data in Figure 3^a

compound	amine ⁺⁰	amine ^{2+/+}	amine ^{3+/2+}	$\text{Re}^{2+/+}$	bpy ^{0/-}	AQ ^{0/-}	AQ ^{-/2-}
Re_2 -TAA	0.46			1.23	-1.76		
Re_2 -OTA	-0.07	0.25	0.65	0.88	-1.88		
AQ-Re-OTA	-0.05	0.21	0.74	0.95	-1.8	-1.29	-1.8
ref				1.37	-1.77		

^aPeak-to-peak separations for the various reversible and quasi-reversible oxidation and reduction processes are given in the Supporting Information (Table S1).

Irreversible rhenium-based oxidations are detected at peak potentials ranging from 1.37 to 0.88 V vs Fc^+/Fc (Table 1), in line with prior reports.^{10a,19} Evidently, the attachment of electron-rich amines (TAA, OTA) to the rhenium complexes makes them easier to oxidize. In Re_2 -TAA (Figure 3, green trace) oxidation of the TAA group occurs at 0.46 V vs Fc^+/Fc as commonly observed,²⁰ and this is a reversible process as long as the voltage sweep does not extend over the rhenium oxidation. In Re_2 -OTA and AQ-Re-OTA two consecutive and reversible one-electron oxidation processes associated with the OTA unit are detected at ca. -0.05 V and near 0.2 V vs Fc^+/Fc (Table 1). A third OTA-based one-electron oxidation process near 0.7 V vs Fc^+/Fc is irreversible. Thus, OTA is a far stronger donor than TAA, and OTA may in fact donate two electrons at less positive potentials than what is required for one-electron oxidation of TAA. Reductions based on the bpy-ligands occur near -1.8 V vs Fc^+/Fc in all four compounds, in line with prior studies.^{9d,19b,c} In AQ-Re-OTA this overlaps with the second one-electron reduction of the AQ moiety; its first one-electron reduction occurs at -1.29 V vs Fc^+/Fc (Table 1).^{8b}

In Figure 4a the spectral changes associated with the addition of increasing amounts of $\text{Cu}(\text{ClO}_4)_2$ to Re_2 -TAA in CH_3CN are shown. $\text{Cu}(\text{ClO}_4)_2$ can be used to oxidize TAA by one electron.^{20a} Below 320 nm the absorbance decreases upon converting Re_2 -TAA to Re_2 -TAA⁺, whereas between 330 and 420 nm it increases. The most prominent feature, however, is a new absorption band centered ~ 770 nm, which is typical for triarylamine monocations.^{9b,20a,21} In Figure 4b the transient absorption spectrum detected after excitation of a 35 μM solution of Re_2 -TAA in CH_3CN at 355 nm is shown. Laser pulses of ~ 10 ns duration were employed, and detection occurred by time-averaging over the first 200 ns immediately after the pulses. Bands at 360 and 770 nm are observed, compatible with the formation of TAA⁺ as the comparison with Figure 4a shows readily. Reduction of the bpy ligand of one of the rhenium complexes is expected to result in a bleach below 300 nm,²² but this cannot be detected because the optical density of the solutions useable for transient absorption spectroscopy is too high in the relevant spectral range. Nevertheless, the formation of a charge-separated state comprised of TAA⁺ and a reduced rhenium complex after photoexcitation of Re_2 -TAA is undisputable. On the basis of the redox potentials from Table 1 and assuming a triplet metal-to-ligand charge transfer (³MLCT) energy of ~ 2.8 eV for the $[\text{Re}(\text{bpy})(\text{CO})_3(\text{py})]^+$ unit, electron transfer from TAA to the photosensitizer is associated with a reaction free energy (ΔG_{ET}^0) of approximately -0.6 eV. In freeze-pump-thaw deoxygenated CH_3CN at 25 °C this charge-separated state has a lifetime of 39 ns (Supporting Information, Figure S1a),

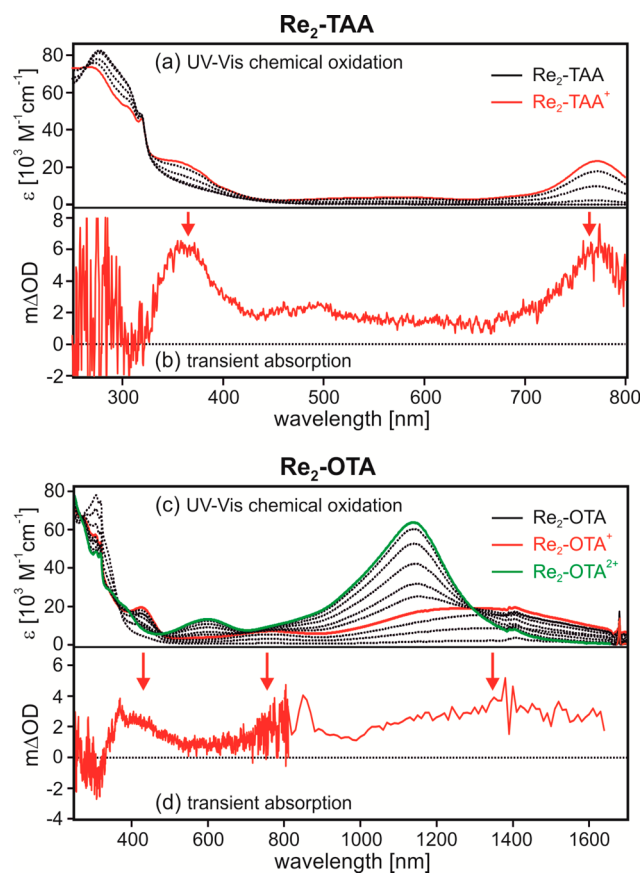


Figure 4. (a) Changes in optical absorption spectra of Re_2 -TAA in CH_3CN upon addition of increasing amounts of $\text{Cu}(\text{ClO}_4)_2$. (b) Transient difference spectrum recorded on a 35 μM solution of Re_2 -TAA in deoxygenated CH_3CN following excitation at 355 nm with laser pulses of ~ 10 ns duration. The spectrum was measured by time-averaging over a 200 ns period following immediately after excitation. (c) Changes in optical absorption spectra of Re_2 -OTA in CH_3CN upon addition of increasing amounts of $\text{Cu}(\text{ClO}_4)_2$. (d) Transient difference spectrum recorded on a 10 μM solution of Re_2 -OTA in deoxygenated CH_3CN under identical conditions as those in (b).

similar to what was reported for other rhenium-based dyads with various redox partners under comparable conditions.²³

Analogous experiments were performed with Re_2 -OTA, and the outcome of the chemical oxidation with $\text{Cu}(\text{ClO}_4)_2$ in CH_3CN is shown in Figure 4c. $\text{Cu}(\text{ClO}_4)_2$ is able to oxidize OTA to OTA⁺ and OTA²⁺.^{20a} The one-electron oxidized form of OTA exhibits absorption maxima at 425, 780, and 1320 nm and thus resembles TAA⁺. By contrast, OTA²⁺ displays absorptions maximizing at 600 and 1140 nm and hence is spectroscopically clearly distinct from OTA⁺, particularly in the near-infrared (NIR) spectral range. In Figure 4d the transient

absorption spectrum of a 10 μM solution of $\text{Re}_2\text{-OTA}$ in CH_3CN recorded under analogous conditions as described above for $\text{Re}_2\text{-TAA}$ is shown. This spectrum shows all the features expected for OTA^+ , and we conclude that the main photoproduct is a charge-separated state comprised of OTA^+ and a reduced rhenium complex ($\Delta G_{\text{ET}}^0 \approx -1.0$ eV), in complete analogy to the $\text{Re}_2\text{-TAA}$ system. In deoxygenated CH_3CN this state has a lifetime of 36 ns (Supporting Information, Figure S1b), very similar to what was found for $\text{Re}_2\text{-TAA}$.

The observation that OTA^+ dominates the transient absorption spectrum in Figure 4d is no surprise. If OTA^{2+} is generated at all, the population of a charge-separated state comprised of two one-electron reduced rhenium complexes and an OTA^{2+} unit is likely to be small compared to the population of the main photoproduct detected in Figure 4d. The reasons for this are simple: Generation of OTA^{2+} requires two-photon excitation, which is inherently less efficient than a one-photon process. In addition, more decay pathways are open for the more energy-storing state comprised of OTA^{2+} and two reduced rhenium complexes than for the simple charge-separated state that dominates the spectrum in Figure 4d. Two-photon processes usually exhibit a quadratic dependence on the laser excitation power.²⁴ Hence, we reasoned that when performing variations in the excitation density we might be able to detect spectral changes that are indicative of OTA^{2+} formation. In Figure 5a the transient absorption spectra

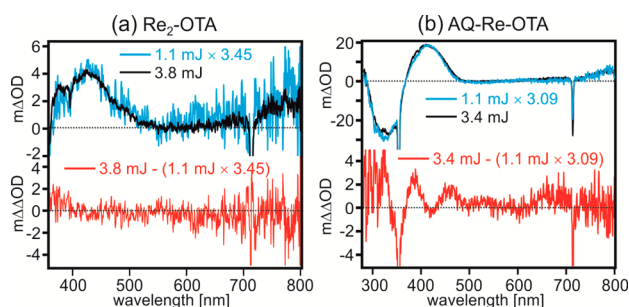


Figure 5. (a) Transient absorption spectra recorded on a 10 μM solution of $\text{Re}_2\text{-OTA}$ in deoxygenated CH_3CN after excitation at 355 nm. Detection occurred by time-averaging over 200 ns immediately after excitation with laser pulses of ~ 10 ns duration. The black and blue spectra were recorded using different laser powers. The blue trace was multiplied by a factor of 3.45 ($= 3.8/1.1$). The red trace is the difference between the black and blue spectra. (b) Analogous sets of data for a 10 μM solution of AQ-Re-OTA in deoxygenated CH_3CN , using a multiplication factor of 3.09 ($= 3.4/1.1$) for the blue trace.

recorded with laser excitation powers of 3.8 (black) and 1.1 (blue) mJ per pulse are shown. The blue trace was multiplied by a factor of 3.45 (the quotient of 3.8 mJ and 1.1 mJ). The red trace is the result of a subtraction of the blue trace from the black spectrum. As seen above (Figure 4c), OTA^{2+} has a significantly higher molar extinction coefficient at 600 nm than that of OTA^+ ; hence, with increasing laser power one could have expected increasing transient absorption at 600 nm. However, this effect cannot be detected in the red difference spectrum of Figure 5a, and we must conclude that there is no evidence for the formation of OTA^{2+} under these conditions. Higher excitation powers lead to sample decomposition, and detection in the NIR spectral range is hampered by the comparatively poor sensitivity of the NIR detector. A further complication might come from the necessity for time-averaging

of the transient absorption spectra and the fact that OTA^{2+} photoproducts might be significantly shorter-lived than the main (OTA^+) photoproduct.

Aside from the multitude of open decay channels for two-electron photoproducts, the two-photon excitation process itself is already challenging even when sufficiently high photon fluxes can be used. One possible pitfall is quenching of the $^3\text{MLCT}$ -excited photosensitizer by energy transfer once OTA^+ is present because the latter has low-energy absorptions. However, luminescence lifetime measurements performed on $\text{Re}_2\text{-TAA}^+$ and $\text{Re}_2\text{-OTA}^+$ in deoxygenated CH_3CN (produced by chemical oxidation with $\text{Cu}(\text{ClO}_4)_2$) demonstrate that the $^3\text{MLCT}$ lifetime in both cases is on the order of 20 ns, similar to what is measured for the $\text{Re}_2\text{-TAA}$ and $\text{Re}_2\text{-OTA}$ compounds before amine oxidation (data not shown). However, even with energy transfer quenching being relatively inefficient, there is still the possibility that once the photoproducts identified on the basis of Figure 4 have been formed via absorption of one photon, the absorption of a second photon by the yet unreacted rhenium center will actually induce (reverse) electron transfer from the $^3\text{MLCT}$ -excited photosensitizer to TAA^+ or OTA^+ .

Compared to the $\text{Re}_2\text{-OTA}$ dyad, the AQ-Re-OTA triad has the advantage that electrons and holes can be separated from each other over a greater distance, potentially leading to longer lifetimes, which in turn will simplify photoproduct detection.^{9b,23c} Its main disadvantage is that it contains only one photosensitizer. Hence, after its initial excitation, formation of a first charge-separated state comprised of OTA^+ and AQ^- coupled to relaxation of the sensitizer to the ground state would have to occur within less than 10 ns, such that the second excitation of the same rhenium complex can still occur within the duration of the same laser pulse.²⁵ On the basis of our own recent studies of triarylamine–ruthenium/osmium–anthraquinone triads this is not an unreasonable expectation because in these triads the charge-separated state containing TAA^+ and AQ^- was formed within ~ 200 ps.^{9b,d} This double-excitation process would resemble the sequence of ground-state absorption and excited-state absorption in upconversion materials, in which the same chromophore is excited twice within the same ~ 10 ns laser pulse.²⁶ For photoinduced two-electron transfer double-excitation with two separate laser pulses has been previously achieved in a system containing $\text{Ru}(\text{bpy})_3^{2+}$ and TiO_2 nanoparticles.^{5b}

Chemical oxidation of AQ-Re-OTA in CH_3CN by $\text{Cu}(\text{ClO}_4)_2$ leads to similar results as for $\text{Re}_2\text{-OTA}$ (Figure 6a). One- and two-electron oxidation products are clearly distinguishable from each other; nearly the same spectral features as in Figure 4c are detected for OTA^+ and OTA^{2+} . The transient absorption spectrum averaged over a 200 ns time window after excitation of a 10 μM solution of AQ-Re-OTA in pure CH_3CN at 355 nm (Figure 6b, black trace) exhibits absorption maxima at 1280, 563, and 428 nm along with a bleach at 330 nm. The bands at 1280 and 428 nm are compatible with formation of OTA^+ , and based on prior studies the absorption at 563 nm and the bleach at 330 nm can be attributed unambiguously to AQ^- .^{8b,9} An increase in laser excitation power from 1.1 to 3.4 mJ per pulse did not result in any changes in the transient absorption spectrum, which could reasonably be interpreted in terms of a manifestation of OTA^{2+} or AQ^{2-} (Figure 5b).

The transient absorption signals for the $\text{AQ}^-\text{-Re-OTA}^+$ state appear immediately after excitation with pulses of ~ 10 ns

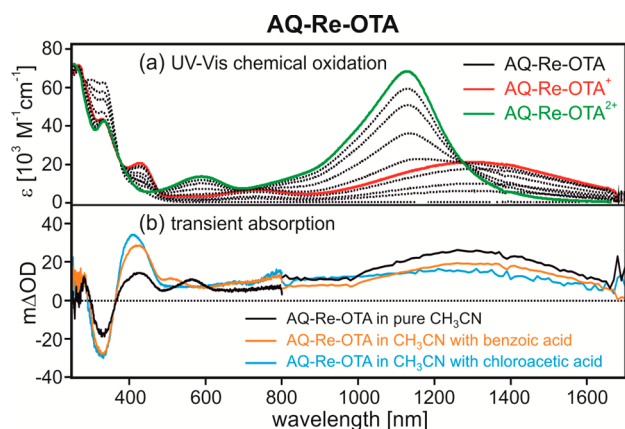


Figure 6. (a) Changes in optical absorption spectra of AQ–Re–OTA in CH_3CN upon addition of increasing amounts of $\text{Cu}(\text{ClO}_4)_2$. (b) Transient difference spectra recorded on a $10 \mu\text{M}$ solution of AQ–Re–OTA in deoxygenated CH_3CN following excitation at 355 nm with laser pulses of $\sim 10 \text{ ns}$ duration. The spectra were recorded by time-averaging over a 200 ns period following immediately after excitation.

duration (Figure 7a), indicating their instantaneous formation. Consequently, the photosensitizer returns to its electronic

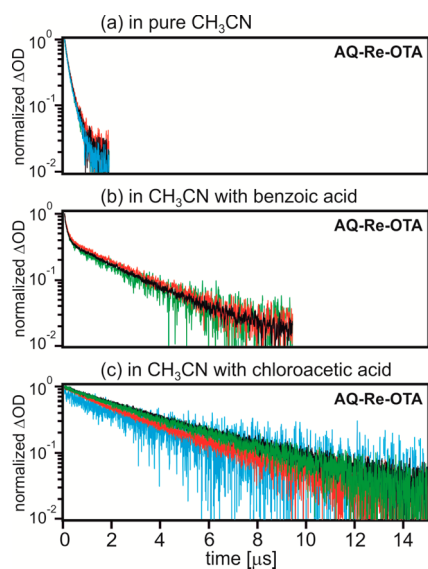


Figure 7. (a) Decays of the transient absorption signals at 790 (red), 565 (green), 428 (blue), and 390 nm (black) of a $10 \mu\text{M}$ solution of AQ–Re–OTA in deoxygenated CH_3CN following excitation at 355 nm with laser pulses of $\sim 10 \text{ ns}$ duration. (b) Transient absorption decays recorded at 790 (red), 670 (green), and 420 nm (black) in an analogous experiment in the presence of 0.2 M benzoic acid. (c) Transient absorption decays recorded at 1240 (red), 790 (green), 675 (blue), and 410 nm (black) in an analogous experiment in presence of 0.2 M chloroacetic acid.

ground state very rapidly and re-excitation with a second photon within the duration of one pulse would indeed appear to be possible, as anticipated above. Irrespective of detection wavelength, the transient absorption signals associated with the AQ^- –Re–OTA $^+$ state exhibit a lifetime of 205 ns in deoxygenated CH_3CN .

Two-electron reduction of quinones occurs with particular ease in protic solvents or, better, in presence of acids because

relatively stable hydroquinones can be formed.^{8,27} Therefore, we explored the photochemistry of the AQ–Re–OTA triad in CH_3CN in presence of 0.2 M benzoic acid and 0.2 M chloroacetic acid; the respective transient absorption spectra are shown as orange and blue traces in Figure 6b. Even in the presence of such high concentrations of organic acids, spectral features clearly attributable to OTA $^+$ can be detected near 410 and 1280 nm , indicating that OTA is not protonated and can still undergo electron transfer under these conditions. Triaryl-amines are poorly basic compared to other tertiary amines due to their propeller-like structure, and evidently this is also the case for OTA (Figure 1). Significant differences between the three transient absorption spectra from Figure 6b occur in the spectral range between 625 and 475 nm : the band detected at 563 nm in pure CH_3CN (black trace), attributed above to AQ^- , shifts to 510 nm in presence of 0.2 M benzoic acid (orange) and finally disappears (or is hidden below the band at 410 nm) in presence of 0.2 M chloroacetic acid (blue). The bleach at 330 nm persists. All transient absorption signals in CH_3CN with 0.2 M benzoic acid decay in a biexponential manner with average lifetimes of 100 and 2250 ns , respectively (Figure 7b, Table 2). In CH_3CN with 0.2 M chloroacetic acid the decays are single-exponential with an average lifetime of 3680 ns (Figure 7c, Table 2).

Table 2. Lifetimes of the Detectable Photoproducts in Deoxygenated Solvents

compound	τ [ns]		
	CH_3CN	CH_3CN 0.2 M $\text{C}_6\text{H}_5\text{COOH}$	CH_3CN 0.2 M ClCH_2COOH
Re_2 –TAA	39		
Re_2 –OTA	36		
AQ–Re–OTA	205	100/2250	3680

The combined observations of anthraquinone-related spectral band-shifts (Figure 6b) and an increase in photoproduct lifetime upon addition of organic acids (Figure 7b,c) are compatible with the formation of the protonated (semi-quinone) form of anthraquinone (AQH).^{8b,28} The occurrence of biexponential decays in the presence of benzoic acid (Figure 7b) with one decay component resembling that detected in pure CH_3CN (205 vs 100 ns , Table 2) and a second component similar to that observed in the presence of 0.2 M chloroacetic acid (2250 vs 3680 ns , Table 2) suggests that the presence of 0.2 M benzoic acid leads to a mixture of AQ^- and AQH photoproducts. The pK_a of AQH in CH_3CN is not known,^{8b} but given the acidity constants reported for benzoic acid and chloroacetic acid in CH_3CN (21.5 vs 18.8),²⁹ it is clear that the latter will protonate AQ^- more readily than benzoic acid. Thus, in the presence of acid, proton-coupled electron transfer (PCET) occurs with our AQ–Re–OTA triad, similar to the electrochemically induced PCET chemistry reported earlier for quinone-based systems.^{8a} Our findings are in line with recent studies in which hydrogen-bond donating solvents (e. g., hexafluoroisopropanol, trifluoroethanol) were found to increase the lifetimes of charge-separated states with quinone acceptors,^{16,28,30} and they are similar to what was observed earlier for the primary charge separation events of bacterial photosynthesis.³¹

SUMMARY AND CONCLUSIONS

The lack of evidence for two-electron photoredox products (OTA^{2+} , AQ^{2-}) in $\text{Re}_2\text{-OTA}$ and AQ-Re-OTA can have several origins. A key factor is the relatively short excitation wavelength (355 nm), which is required to excite these rhenium(I) tricarbonyl diimine based systems. This is detrimental in several respects: First of all, light of this wavelength does not lead to selective excitation of the photosensitizer but (based on the UV-vis spectra in Figure 2) occurs at least partly into absorptions localized on OTA and AQ. Second, the photoredox product OTA^+ has a large molar extinction coefficient at 355 nm (Figure 4c, Figure 6a); consequently, once a first photoinduced electron transfer step has occurred, excitation of OTA^+ might interfere with the desired processes that would lead to OTA^{2+} . Third, the photodamage threshold of the investigated molecules for 355 nm excitation is relatively low, and the phototriggered loss of CO ligands at the rhenium photosensitizer is a well-known phenomenon.³² We consider the use of a photosensitizer that permits excitation at longer wavelengths of pivotal importance for our future endeavors of detecting two-electron photoredox products in purely molecular (nanoparticle-free) systems. Obviously this remains a significant challenge because numerous decay channels are open for two-photon excited intermediates and two-electron photoredox products,^{4b,5b,c,6a,33} and it is difficult to design a system in which undesired (energy-wasting) electron and energy transfer processes can be efficiently suppressed. Pump-pump-probe experiments that make use of two temporally delayed excitation pulses (possibly even of different wavelengths) would certainly represent a major advantage, particularly when performed with high temporal resolution (<10 ns) to detect very short-lived photoproducts.^{5c,6e} In our specific cases explored in this study, the applicable photon flux was likely too low. We estimate that for the useable laser excitation powers and concentrations, the photon flux was on the order of 1–2 photons per molecule per pulse. With sufficiently high photon fluxes a possible additional problem is two-photon ionization of the rhenium(I) photosensitizer (producing solvated electrons), similar to what has been previously observed for $\text{Ru}(\text{bpy})_3^{2+}$.³⁴

In principle, the consecutive 2-fold excitation of the photosensitizer in the AQ-Re-OTA triad should be possible within the duration of a 10 ns laser pulse because the $\text{AQ}^-\text{-Re-OTA}^+$ state is formed very rapidly (Figure 7).²⁵ In closely related ruthenium- and osmium-based triads full charge-separation with an electron on the acceptor and a hole on the donor took as little as ~200 ps.^{9d,35} The use of one single photosensitizer for accessing two-electron photoredox products, albeit certainly challenging, should therefore in principle be possible, at least when using relatively long (~10 ns) and sufficiently strong excitation pulses.

Our study of the AQ-Re-OTA triad shows that anthraquinone monoanion (AQ^-) and the protonated semiquinone form (AQH) are distinguishable by UV-vis transient absorption spectroscopy. This might be useful for studies of photoinduced PCET with quinones.³⁶ Thus, the PCET chemistry of quinones can potentially be exploited for accumulation of multiple electrons on such units. We are currently exploring this possibility.

EXPERIMENTAL SECTION

Synthesis and Product Characterization. Commercially available chemicals were used as received. Dichloromethane, diethyl ether,

and tetrahydrofuran (THF) were dried in a solvent purification system from Innovative Technology. Dry toluene was bought from Sigma-Aldrich (crown-capped, over molecular sieve). Silicycle silica gel (40–63 mm) was used for column chromatography. Thin-layer chromatography was performed on silica gel plates (60 F_{254}) from Merck.

Compound 2. For the synthesis of this molecule we followed a previously published procedure.^{7c} Commercially available bis(4-bromophenyl)amine **1** (2.00 g, 6.12 mmol), 4-(*N,N*-dimethylamino)pyridine (149.5 mg, 1.22 mmol), and di-*tert*-butyl dicarbonate (2.11 mg, 9.17 mmol) were dissolved in dry THF (15 mL) under N_2 . The yellow solution was heated to reflux for 3 h. After it was cooled to room temperature and the subsequent removal of the solvent on a rotary evaporator, the crude orange solid was filtered over SiO_2 with a 2:1 (v:v) pentane/dichloromethane eluent mixture, which afforded the pure product as a white solid (2.60 g, 6.09 mmol, ~100%). $^1\text{H NMR}$ (400 MHz, CDCl_3) δ : 7.45–7.41 (m, 4H), 7.08–7.04 (m, 4 H), 1.44 (s, 9 H).

Compound 4. This synthesis was performed by adapting a previously published protocol.^{7c} Compound **2** (1.00 g, 2.34 mmol), commercially available dianisylamine **3**, (1.34 g, 5.86 mmol), $^t\text{BuONa}$ (4.5 g, 46.8 mmol), $\text{Pd}(\text{dba})_2$ (67.2 mg, 0.12 mmol), and $(\text{HP}^t\text{Bu}_3)\text{BF}_4$ (34.2 mg, 0.12 mmol) were dissolved in dry and deoxygenated toluene (30 mL) under nitrogen. The reaction mixture was heated to 120 °C for 19 h. Water (100 mL) was added to the cooled mixture, and the aqueous phase was extracted with dichloromethane (3 × 50 mL). The combined organic phases were dried over anhydrous MgSO_4 , and subsequently the solvent was evaporated. Column chromatography on silica gel with dichloromethane as the eluent gave the product as a beige solid (1.42 g, 1.96 mmol, 84%). $^1\text{H NMR}$ (400 MHz, acetone- d_6) δ : 7.09–7.05 (m, 4 H), 7.04–7.00 (m, 8 H), 6.91–6.87 (m, 8 H), 6.82–6.78 (m, 4 H), 3.78 (s, 12 H), 1.41 (s, 9 H).

Compound 5. This reaction step was performed following a published procedure.¹² Compound **4** (2.00 g, 2.76 mmol) was dissolved in acetone (40 mL) under nitrogen. Trifluoroacetic acid (TFA, 10 mL, 0.13 mol) was added drop by drop, and the solution was stirred at room temperature overnight. Then the reaction mixture was evaporated to dryness. Column chromatography on basic alumina with ethyl acetate as the eluent yielded the product as a beige solid (1.70 g, 2.73 mmol, 99%). Single crystals for X-ray diffraction were obtained from acetone solution by slow evaporation. $^1\text{H NMR}$ (400 MHz, acetone- d_6 with a drop of TFA) δ : 7.40–7.37 (m, 4 H), 7.18–7.14 (m, 8 H), 6.98–6.94 (m, 8 H), 6.87–6.83 (m, 4 H), 3.80 (s, 12 H).

Compound 8. 1,3,5-Tribromobenzene **6** (0.50 g, 1.59 mmol), commercial pyridine-4-boronic acid hydrate **7** (586.3 mg, 4.77 mmol), and Na_2CO_3 (3.00 g, 28.3 mmol) were suspended in a mixture comprised of water (10 mL) and THF (20 mL). After deoxygenating the mixture by bubbling N_2 for 30 min, $\text{Pd}(\text{PPh}_3)_4$ (184 mg, 0.16 mmol) was added. Then the reaction mixture was deoxygenated further, and finally it was heated to 90 °C for 24 h. After it was cooled to room temperature, water was added (50 mL), and the mixture was extracted with dichloromethane (3 × 50 mL). The combined organic phases were dried over anhydrous Na_2SO_4 , and the solvents were removed on a rotary evaporator. Purification by column chromatography on silica gel using dichloromethane with 2% of triethylamine yielded the desired product as a light green solid (0.18 g, 0.58 mmol, 36%). $^1\text{H NMR}$ (400 MHz, CDCl_3) δ : 8.75–8.69 (m, 4 H), 7.83 (d, 2 H, $J = 1.6$ Hz), 7.77 (t, 1 H, $J = 1.6$ Hz), 7.54–7.49 (m, 4 H).

Ligand 9. Compound **8** (180.5 mg, 0.58 mmol), compound **5** (0.30 g, 0.48 mmol), $^t\text{BuONa}$ (1.11 g, 11.6 mmol), $\text{Pd}(\text{dba})_2$ (13.8 mg, 0.02 mmol), and $(\text{HP}^t\text{Bu}_3)\text{BF}_4$ (6.90 mg, 0.02 mmol) were dissolved in dry and deoxygenated toluene (25 mL) under N_2 . The reaction mixture was heated to 125 °C for 19 h. After it cooled to room temperature, water (100 mL) was added, and the mixture was extracted with dichloromethane (3 × 50 mL). After drying over anhydrous MgSO_4 the organic solvents were evaporated, and the crude product was purified by column chromatography on silica gel using dichloromethane with 2% triethylamine as the eluent. Subsequent recrystallization from hexane gave the product as an olive-green solid (292 mg, 0.34 mmol, 71%). $^1\text{H NMR}$ (400 MHz, CDCl_3) δ : 8.66 (d, 4 H, $J =$

4.7 Hz), 7.44 (d, 4 H, $J = 6.2$ Hz), 7.29 (s, 3 H), 7.08–7.04 (m, 8 H), 7.02–6.99 (m, 4 H), 6.91–6.87 (m, 4 H), 6.85–6.81 (m, 8 H), 3.79 (s, 12 H).

$\text{Re}_2\text{-OTA}$. Ligand **9** (0.10 g, 0.12 mmol) and $[\text{Re}(\text{bpy})(\text{CO})_3\text{OTf}]$ (148.2 mg, 0.26 mmol)¹³ were dissolved in a mixture of methanol (10 mL) and chloroform (3 mL). After deoxygenating for 25 min, the reaction mixture was heated to 85 °C for 1.5 d. Then the solvents were evaporated, and the crude product was purified by column chromatography on silica gel. The eluent was a mixture of pure acetone, deionized water, and saturated aqueous KNO_3 solution in the ratio of 200:9:1 (v/v/v). An orange solid was obtained, and this was dissolved in water (50 mL) and extracted with dichloromethane (3×50 mL). The combined organic phases were dried over anhydrous Na_2SO_4 prior to evaporating the solvent. The solid residue was recrystallized from hexane, yielding the desired complex in the form of its nitrate salt as a yellow-brownish solid (83 mg, 0.04 mmol, 37%). ¹H NMR (400 MHz, CD_3CN) δ : 9.23 (ddd, 4 H, $J = 5.5, 1.6, 0.7$ Hz), 8.40 (dt, 4 H, $J = 8.3, 1.1$ Hz), 8.27 (td, 4 H, $J = 7.9, 1.6$ Hz), 8.23–8.19 (m, 4 H), 7.80 (ddd, 4 H, $J = 7.7, 5.5, 1.3$ Hz), 7.41–7.36 (m, 4 H), 7.20 (s, 1 H), 7.12 (s, 2 H), 6.88 (m, 24 H), 3.78 (s, 12 H). ESI-MS (m/z) calculated for $\text{C}_{82}\text{H}_{63}\text{N}_9\text{O}_{10}\text{Re}_2$: 853.6902; found: 853.6915. Elemental analysis calculated for $\text{C}_{82}\text{H}_{63}\text{N}_{11}\text{O}_{16}\text{Re}_2 \cdot 3\text{H}_2\text{O}$ (%): C, 52.25; H, 3.69; N, 8.17; found: C, 52.14; H, 3.79; N, 8.09.

Ligand **10**. Compound **8** (66 mg, 0.21 mmol), dianisylamine (58.3 mg, 0.25 mmol), tBuONa (404 mg, 4.2 mmol), $\text{Pd}(\text{dba})_2$ (6 mg, 0.01 mmol), and $(\text{HP}^t\text{Bu}_3)\text{BF}_4$ (3 mg, 0.01 mmol) were dissolved in dry and deoxygenated toluene (5 mL) under N_2 . This mixture was heated to 100 °C for 22.5 h. After cooling to room temperature, water (50 mL) was added, and the mixture was extracted with dichloromethane (3×50 mL). The combined organic phases were dried over anhydrous Na_2SO_4 and then evaporated. Column chromatography on silica gel occurred with dichloromethane containing 1% triethylamine. This procedure afforded the product as a beige solid (80 mg, 0.17 mmol, 83%). ¹H NMR (400 MHz, CDCl_3) δ : 8.62 (m, 4 H), 7.41 (m, 4 H), 7.29 (t, 1 H, $J = 1.6$ Hz), 7.20 (d, 2 H, $J = 1.6$ Hz), 7.16–7.12 (m, 4 H), 6.90–6.86 (m, 4 H), 3.82 (s, 6 H).

$\text{Re}_2\text{-TAA}$. Ligand **10** (0.10 g, 0.22 mmol) and $[\text{Re}(\text{bpy})(\text{CO})_3\text{OTf}]$ (276 mg, 0.48 mmol)¹³ were dissolved in methanol (10 mL). Prior to heating to 85 °C overnight, the reaction mixture was deoxygenated by bubbling N_2 gas during 45 min. After evaporating to dryness, the crude product was purified by column chromatography using the same conditions as described above for $\text{Re}_2\text{-OTA}$. An orange fraction was collected and dissolved in water (50 mL). This solution was extracted with dichloromethane (3×50 mL), and the combined organic phases were dried over Na_2SO_4 and evaporated. Recrystallization from hexane gave the desired complex in the form of its nitrate salts as an orange solid (161 mg, 0.11 mmol, 50%). ¹H NMR (400 MHz, CD_3CN) δ : 9.21 (ddd, 4 H, $J = 5.5, 1.6, 0.8$ Hz), 8.37 (dt, 4 H, $J = 8.3, 1.0$ Hz), 8.25 (td, 4 H, $J = 7.9, 1.5$ Hz), 8.20–8.15 (m, 4 H), 7.77 (ddd, 4 H, $J = 7.6, 5.5, 1.3$ Hz), 7.37–7.32 (m, 4 H), 7.19 (t, 1 H, $J = 1.6$ Hz), 7.07–7.02 (m, 4 H), 6.97 (d, 2 H, $J = 1.6$ Hz), 6.89–6.84 (m, 4 H), 3.75 (s, 6 H). ESI-MS (m/z) calculated for $\text{C}_{56}\text{H}_{41}\text{N}_7\text{O}_8\text{Re}_2$: 656.6061; found: 656.6075. Elemental analysis calculated for $\text{C}_{56}\text{H}_{41}\text{N}_9\text{O}_{14}\text{Re}_2 \cdot 2\text{H}_2\text{O}$ (%): C, 45.68; H, 3.08; N, 8.56; found: C, 45.62; H, 3.21; N, 8.63.

Compound **13**. 2-Bromoanthraquinone **11** (3.32 g, 11.6 mmol), 4-trimethylsilyl-2,5-dimethylphenylboronic acid **12** (3.08 g, 13.9 mmol),^{11d} and Na_2CO_3 (3.67 g, 34.7 mmol) were suspended in a mixture of water (12 mL), ethanol (10 mL), and toluene (60 mL). After bubbling N_2 gas during 15 min, $\text{Pd}(\text{PPh}_3)_4$ (1.33 g, 1.16 mmol) was added, and the reaction mixture was further deoxygenated prior to refluxing for 1.5 d. After it was cooled to room temperature, deionized water (100 mL) was added, and the mixture was extracted with dichloromethane (3×50 mL). The combined organic phases were dried over anhydrous Na_2SO_4 and then evaporated to dryness. Column chromatography on silica gel occurred with a pentane–dichloromethane 1:1 (v/v) mixture. This procedure afforded the product as a yellow solid (4.44 g, 11.6 mmol, ~100%). ¹H NMR (400 MHz, CDCl_3) δ : 8.38–8.32 (m, 3 H), 8.30 (d, 1 H, $J = 1.8$ Hz), 7.82

(m, 2 H), 7.79–7.76 (dd, 1 H, $J = 8.0, 1.9$ Hz), 7.40 (s, 1 H), 7.11 (s, 1 H), 2.49 (s, 3 H), 2.30 (s, 3 H), 0.38 (s, 9 H).

Compound **14**. Compound **13** (1.97 g, 5.12 mmol) was dissolved in dichloromethane (10 mL) under N_2 and cooled to 0 °C. A solution of ICl (563 μL , 10.8 mmol) in acetonitrile (40 mL) was added very slowly, and the resulting suspension was stirred at 0 °C for 15 min. Then the ice bath was removed, and the reaction mixture was stirred at room temperature overnight. Following addition of aqueous $\text{Na}_2\text{S}_2\text{O}_3$ (5%, 200 mL), the mixture was extracted with dichloromethane (3×50 mL). The combined organic phases were washed with water (50 mL) and then dried over anhydrous Na_2SO_4 . After evaporation to dryness a yellow solid was obtained (2.2 g, 5.12 mmol, ~100%). ¹H NMR (400 MHz, CDCl_3) δ : 8.37–8.31 (m, 3 H), 8.25 (d, 1 H, $J = 1.8$ Hz), 7.85–7.80 (m, 2 H), 7.79 (s, 1 H), 7.74–7.72 (dd, 1 H, $J = 8.0, 1.8$ Hz), 7.14 (s, 1 H), 2.45 (s, 3 H), 2.23 (s, 3 H).

Ligand **16**. Compound **14** (820 mg, 1.87 mmol) and 5-(tri(*n*-butyl)stannyl)-2,2'-bipyridine **15** (1.00 g, 2.25 mmol)^{11d,15} were dissolved in *m*-xylene (80 mL). After bubbling N_2 gas for 30 min, $\text{Pd}(\text{PPh}_3)_4$ (108 mg, 0.09 mmol) was added, and the reaction mixture was further deoxygenated prior to heating to 150 °C for 70 h. Water (150 mL) was added to the cooled black suspension. This mixture was extracted with dichloromethane (3×50 mL). The combined organic phases were dried over anhydrous MgSO_4 prior to solvent evaporation. The crude product was purified by column chromatography on silica gel using first pure dichloromethane, then dichloromethane with 1% triethylamine as the eluent. Subsequent recrystallization from hexane gave a yellow solid (640 mg, 1.37 mmol, 73%). ¹H NMR (400 MHz, CDCl_3) δ : 8.73 (ddd, 2 H, $J = 5.5, 2.0, 0.9$ Hz), 8.50 (dd, 1 H, $J = 8.1, 0.8$ Hz), 8.46 (dt, 1 H, $J = 8.0, 1.1$ Hz), 8.40 (d, 1 H, $J = 8.0$ Hz), 8.38–8.32 (m, 3 H), 7.89–7.80 (m, 6 H), 7.34 (ddd, 1 H, $J = 7.5, 4.8, 1.8$ Hz), 7.27 (s, 1 H), 2.36 (m, 6 H).

Complex **17**. Ligand **16** (0.15 g, 0.32 mmol) and $\text{Re}(\text{CO})_5\text{Cl}$ (116 mg, 0.32 mmol) were suspended in toluene (25 mL) and heated to reflux overnight. After it was cooled to room temperature, the yellow precipitate was filtered, washed with diethyl ether, and finally dried in vacuum (225 mg, 0.29 mmol, 91%). ¹H NMR (400 MHz, CDCl_3) δ : 9.13–9.07 (m, 2 H), 8.42 (d, 1 H, $J = 8.0$ Hz), 8.38–8.32 (m, 3 H), 8.26 (dd, 2 H, $J = 9.7, 8.0$ Hz), 8.11 (ddd, 2 H, $J = 8.6, 6.9, 1.9$ Hz), 7.87–7.80 (m, 3 H), 7.57 (ddd, 1 H, $J = 7.6, 5.5, 1.2$ Hz), 7.30 (d, 2 H, $J = 6.6$ Hz), 2.39 (m, 6 H).

Complex **18**. Complex **17** (201 mg, 0.26 mmol) was suspended in dry dichloromethane (15 mL). Trifluoromethanesulfonic acid (1.50 mL, 17 mmol) was added dropwise at room temperature, and the resulting homogeneous solution was stirred for 2 h at this temperature. Then diethyl ether was added slowly, and the product precipitated as a yellow solid. After storing the mixture in the refrigerator overnight, the yellow solid was filtered, washed with diethyl ether, and finally dried in vacuum (190 mg, 0.21 mmol, 83%). ¹H NMR (400 MHz, CDCl_3) δ : 9.16–9.10 (m, 2 H), 8.42 (dd, 1 H, $J = 8.0, 2.0$ Hz), 8.39–8.32 (m, 3 H), 8.29 (m, 2 H), 8.24–8.15 (m, 2 H), 7.87–7.79 (m, 3 H), 7.66 (ddd, 1 H, $J = 7.6, 5.4, 1.3$ Hz), 7.30 (m, 2 H), 2.42–2.35 (m, 6 H).

Compound **20**. Pyridine-4-boronic acid hydrate **7** (1.00 g, 5.14 mmol), 1-bromo-4-trimethylsilyl-2,5-dimethylbenzene **19** (1.37 g, 6.17 mmol),^{11c} and Na_2CO_3 were suspended in a mixture of water, ethanol, and toluene (8:6:20; v/v/v) under N_2 . After bubbling N_2 gas through the suspension for 20 min, $\text{Pd}(\text{PPh}_3)_4$ (60 mg, 0.05 mmol) was added, and the suspension was further deoxygenated by bubbling N_2 for 10 min prior to refluxing for 1.5 d. Water (100 mL) was added to the cooled reaction mixture, and then the mixture was extracted with dichloromethane (3×50 mL). After drying over anhydrous MgSO_4 the combined organic phases were evaporated, and the crude product was purified by column chromatography on silica gel. The eluent was a mixture of pentane and dichloromethane (2:1, v/v) containing 1% triethylamine. This procedure afforded the desired product as a pale yellow solid (1.30 g, 5.09 mmol, 99%). ¹H NMR (400 MHz, CDCl_3) δ : 8.65–8.63 (m, 2 H), 7.37 (s, 1 H), 7.27–7.26 (m, 2 H), 7.02 (s, 1 H), 2.46 (s, 3 H), 2.26 (s, 3 H), 0.36 (s, 9 H).

Compound **21**. Compound **20** (1.30 g, 5.09 mmol) was dissolved in dichloromethane (5 mL) under N_2 . After this solution cooled to 0 °C, a solution of ICl (520 μL , 10.2 mmol) in acetonitrile (20 mL) was

added drop by drop. The reaction mixture was stirred at room temperature overnight. Then saturated aqueous $\text{Na}_2\text{S}_2\text{O}_3$ (200 mL) was added, and the product was extracted with dichloromethane (3×50 mL). The combined organic phases were dried over Na_2SO_4 , and then the solvents were removed on a rotary evaporator. Purification occurred by passing the crude product through some silica gel and by washing with an eluent mixture comprised of pentane and dichloromethane (2:1, v/v) with 1% triethylamine. This gave the pure product as a beige solid (1.52 g, 4.92 mmol, 97%). ^1H NMR (400 MHz, CDCl_3) δ : 8.68–8.61 (m, 2 H), 7.76 (s, 1 H), 7.25–7.18 (m, 2 H), 7.06 (s, 1 H), 2.43 (s, 3 H), 2.19 (s, 3 H).

Ligand 22. Compound 21 (177 mg, 0.57 mmol), amine 5 (429 mg, 0.69 mmol), $^t\text{BuOK}$ (1.28 g, 11.4 mmol), $\text{Pd}(\text{dba})_2$ (33 mg, 0.06 mmol), and $(\text{HP}^t\text{Bu}_3)\text{BF}_4$ (16.5 mg, 0.06 mmol) were dissolved in dry and deoxygenated toluene (15 mL) under N_2 . This reaction mixture was heated to 100 °C for 2.5 d. Deionized water (150 mL) was then added to the cooled mixture, and the product was extracted with dichloromethane (3×50 mL). After it was dried over anhydrous Na_2SO_4 and subsequent solvent evaporation, the crude product was purified by column chromatography on silica gel. At first, the eluent was pure dichloromethane, and later dichloromethane with 1% triethylamine was used. This procedure afforded the product as a brownish solid (0.43 g, 0.53 mmol, 94%). ^1H NMR (400 MHz, CDCl_3) δ : 8.64–8.61 (m, 2 H), 7.29–7.26 (m, 2 H), 7.06–6.99 (m, 10 H), 6.87–6.77 (m, 16 H), 3.78 (s, 12 H), 2.20 (s, 3 H), 2.05 (s, 3 H).

AQ–Re–OTA. Complex 18 (81 mg, 0.08 mmol) and ligand 22 (74 mg, 0.10 mmol) were suspended in a mixture of methanol (5 mL) and chloroform (5 mL). Prior to refluxing for 43 h the reaction mixture was deoxygenated by bubbling N_2 gas for 20 min. Then the solvents were evaporated, and the solid residue was subjected to column chromatography on silica gel. At first the eluent was dichloromethane with 1% methanol, followed by dichloromethane with 3% methanol. The product was further purified by dissolving in a minimal amount of dichloromethane and then precipitated by diethyl ether. This procedure afforded the pure product as a dark orange solid (64 mg, 0.04 mmol, 47%). ^1H NMR (400 MHz, CD_3CN) δ : 9.27–9.23 (m, 1 H), 9.19 (d, 1 H, $J = 1.7$ Hz), 8.44 (dd, 2 H, $J = 8.2, 4.2$ Hz), 8.35–8.32 (m, 1 H), 8.31–8.24 (m, 7 H), 7.88 (dt, 3 H, $J = 6.8, 1.5$ Hz), 7.83–7.77 (m, 1 H), 7.44 (s, 1 H), 7.37 (s, 1 H), 7.24 (s, 2 H), 6.86 (s_{broad}, 26 H), 3.73 (s, 12 H), 2.35 (m, 12 H). ESI-MS (m/z) calculated for $\text{C}_{88}\text{H}_{70}\text{N}_6\text{O}_9\text{Re}$: 1541.4675; found: 1541.4774. Elemental analysis calculated for $\text{C}_{88}\text{H}_{70}\text{F}_3\text{N}_6\text{O}_{12}\text{ReS}_2\text{Et}_2\text{O}$ (%): C, 63.29; H, 4.57; N, 4.76; found: C, 63.01; H, 4.68; N, 5.11.

X-ray Crystallography. Crystal data for 5: formula $\text{C}_{40}\text{H}_{37}\text{N}_3\text{O}_4$, $M = 623.75$, $F(000) = 1320$, green block, size $0.080 \times 0.190 \times 0.330$ mm³, orthorhombic, space group $Pccn$, $Z = 4$, $a = 10.2046(8)$ Å, $b = 15.4020(12)$ Å, $c = 20.5009(16)$ Å, $\alpha = 90^\circ$, $\beta = 90^\circ$, $\gamma = 90^\circ$, $V = 3222.2(4)$ Å³, $D_{\text{calc}} = 1.286$ Mg·m⁻³. The crystal was measured on a Bruker Kappa Apex2 diffractometer at 123 K using graphite-monochromated Cu $K\alpha$ radiation with $\lambda = 1.54178$ Å, $\Theta_{\text{max}} = 68.340^\circ$. Minimal/maximal transmission 0.88/0.95, $\mu = 0.665$ mm⁻¹. The Apex2 suite has been used for data collection and integration.³⁷ From a total of 40 707 reflections, 2937 were independent (merging at $r = 0.055$). From these, 2910 were considered as observed ($I > 2.0\sigma(I)$) and were used to refine 215 parameters. The structure was solved by charge flipping using the program Superflip.³⁸ Least-squares refinement against F was carried out on all non-hydrogen atoms using the program CRYSTALS.³⁹ $R = 0.0349$ (observed data), $wR = 0.0384$ (all data), $\text{GOF} = 1.0472$. Minimal/maximal residual electron density = $-0.15/0.22$ e Å⁻³. Chebychev polynomial weights were used to complete the refinement.⁴⁰ Plots were produced using Mercury.⁴¹ Additional crystallographic data are available in the Supporting Information.

Methods and Equipment. NMR spectra were measured on a 400 MHz Bruker Avance III instrument. Chemical shifts are reported in ppm referenced to residual solvent resonances. High-resolution mass spectra were recorded on a Bruker maxis 4G QTOF ESI spectrometer, and elemental analysis was performed using a Vario Micro Cube instrument from Elementar. Optical absorption spectra were recorded

on a Cary 5000 UV–vis–NIR spectrophotometer from Varian. For steady-state luminescence spectroscopy a Fluorolog-322 instrument from Horiba Jobin-Yvon was used. Cyclic voltammetry experiments were performed with a Versastat3–200 potentiostat from Princeton Applied Research using a conventional three-electrode setup. A glassy carbon disk served as a working electrode, and two silver wires were used as counter and quasi-reference electrodes, respectively. Dry, argon-saturated acetonitrile with 0.1 M tetrabutylammonium hexafluorophosphate (TBAPF_6) as supporting electrolyte was used in all cases. Transient absorption spectroscopy was measured on an LP920-KS spectrophotometer from Edinburgh Instruments, equipped with an iCCD camera from Andor and an R928 photomultiplier or an NIR 301/2 (InGaAs) detector (900–1650 nm, ~ 100 ns response time). The frequency-tripled output of a Quantel Brilliant b laser was used for excitation. The duration of the laser excitation pulses was approximately 10 ns, the repetition rate was 10 Hz. Transient absorption spectra were time-averaged over a duration of 200 ns directly after excitation. Quartz cuvettes from Starna were employed for all optical spectroscopic experiments.

■ ASSOCIATED CONTENT

Supporting Information

X-ray crystallographic data for compound 5 in CIF format. NMR and high-resolution ESI mass spectra, additional transient absorption data. This material is available free of charge via the Internet at <http://pubs.acs.org>. Crystallographic data (excluding structure factors) for the structure in this paper were deposited with the Cambridge Crystallographic Data Center; the deposition number is 1011917. Copies of the data can be obtained, free of charge, on application to the CCDC, 12 Union Road, Cambridge CB2 1EZ, UK [fax: +44–1223–336033 or e-mail: deposit@ccdc.cam.ac.uk].

■ AUTHOR INFORMATION

Corresponding Author

*E-mail: oliver.wenger@unibas.ch.

Author Contributions

The manuscript was written through contributions of all authors. All authors have given approval to the final version of the manuscript.

Notes

The authors declare no competing financial interest.

■ ACKNOWLEDGMENTS

This work was supported by the Swiss NSF (Grant No. 200021_146231/1). Support from COST action CM1202 is acknowledged.

■ REFERENCES

- (1) Balzani, V. *Electron transfer in chemistry*; VCH Wiley: Weinheim, Germany, 2001; Vol. 3.
- (2) (a) Gray, H. B.; Winkler, J. R. *Proc. Natl. Acad. Sci. U. S. A.* **2005**, *102*, 3534. (b) Cordes, M.; Giese, B. *Chem. Soc. Rev.* **2009**, *38*, 892.
- (c) Closs, G. L.; Miller, J. R. *Science* **1988**, *240*, 440.
- (3) (a) Wasielewski, M. R. *Chem. Rev.* **1992**, *92*, 435. (b) Guldi, D. M. *Chem. Soc. Rev.* **2002**, *31*, 22. (c) Fukuzumi, S. *Phys. Chem. Chem. Phys.* **2008**, *10*, 2283.
- (4) (a) Gray, H. B.; Maverick, A. W. *Science* **1981**, *214*, 1201. (b) Magnuson, A.; Anderlund, M.; Johansson, O.; Lindblad, P.; Lomoth, R.; Polivka, T.; Ott, S.; Stensjö, K.; Styring, S.; Sundström, V.; Hammarström, L. *Acc. Chem. Res.* **2009**, *42*, 1899.
- (5) (a) Knowles, K. E.; Peterson, M. D.; McPhail, M. R.; Weiss, E. A. *J. Phys. Chem. C* **2013**, *117*, 10229. (b) Karlsson, S.; Boixel, J.; Pellegrin, Y.; Blart, E.; Becker, H. C.; Odobel, F.; Hammarström, L. *Faraday Discuss.* **2012**, *155*, 233. (c) Karlsson, S.; Boixel, J.; Pellegrin,

Y.; Blart, E.; Becker, H. C.; Odobel, F.; Hammarström, L. *J. Am. Chem. Soc.* **2010**, *132*, 17977.

(6) (a) Pellegrin, Y.; Odobel, F. *Coord. Chem. Rev.* **2011**, *255*, 2578. (b) Matt, B.; Fize, J.; Moussa, J.; Amouri, H.; Pereira, A.; Artero, V.; Izzet, G.; Proust, A. *Energy Environ. Sci.* **2013**, *6*, 1504. (c) Manbeck, G. F.; Brewer, K. J. *Coord. Chem. Rev.* **2013**, *257*, 1660. (d) O'Neil, M. P.; Niemczyk, M. P.; Svec, W. A.; Gosztola, D.; Gaines, G. L.; Wasielewski, M. R. *Science* **1992**, *257*, 63. (e) Imahori, H.; Hasegawa, M.; Taniguchi, S.; Aoki, M.; Okada, T.; Sakata, Y. *Chem. Lett.* **1998**, 721. (f) Klein, J. H.; Sunderland, T. L.; Kaufmann, C.; Holzapfel, M.; Schmiedel, A.; Lambert, C. *Phys. Chem. Chem. Phys.* **2013**, *15*, 16024. (g) Zedler, L.; Kupfer, S.; de Moraes, I. R.; Wachtler, M.; Beckert, R.; Schmitt, M.; Popp, J.; Rau, S.; Dietzek, B. *Chem.—Eur. J.* **2014**, *20*, 3793.

(7) (a) Ito, A.; Yokoyama, Y.; Aihara, R.; Fukui, K.; Eguchi, S.; Shizu, K.; Sato, T.; Tanaka, K. *Angew. Chem., Int. Ed.* **2010**, *49*, 8205. (b) Yang, T.-F.; Chiu, K. Y.; Cheng, H.-C.; Lee, Y. W.; Kuo, M. Y.; Su, Y. O. *J. Org. Chem.* **2012**, *77*, 8627. (c) Hirao, Y.; Ino, H.; Ito, A.; Tanaka, K.; Kato, T. *J. Phys. Chem. A* **2006**, *110*, 4866. (d) Yan, X. Z.; Pawlas, J.; Goodson, T.; Hartwig, J. F. *J. Am. Chem. Soc.* **2005**, *127*, 9105.

(8) (a) Gupta, N.; Linschitz, H. *J. Am. Chem. Soc.* **1997**, *119*, 6384. (b) Babaei, A.; Connor, P. A.; McQuillan, A. J.; Umapathy, S. *J. Chem. Educ.* **1997**, *74*, 1200. (c) Quan, M.; Sanchez, D.; Wasylkiw, M. F.; Smith, D. K. *J. Am. Chem. Soc.* **2007**, *129*, 12847.

(9) (a) Opperman, K. A.; Mecklenburg, S. L.; Meyer, T. J. *Inorg. Chem.* **1994**, *33*, 5295. (b) Hankache, J.; Wenger, O. S. *Chem. Commun.* **2011**, *47*, 10145. (c) Lewis, F. D.; Thazhathveetil, A. K.; Zeidan, T. A.; Vura-Weis, J.; Wasielewski, M. R. *J. Am. Chem. Soc.* **2010**, *132*, 444. (d) Hankache, J.; Niemi, M.; Lemmetyinen, H.; Wenger, O. S. *Inorg. Chem.* **2012**, *51*, 6333.

(10) (a) Schanze, K. S.; MacQueen, D. B.; Perkins, T. A.; Cabana, L. A. *Coord. Chem. Rev.* **1993**, *122*, 63. (b) Connick, W. B.; Di Bilio, A. J.; Hill, M. G.; Winkler, J. R.; Gray, H. B. *Inorg. Chim. Acta* **1995**, *240*, 169. (c) Slone, R. V.; Yoon, D. I.; Calhoun, R. M.; Hupp, J. T. *J. Am. Chem. Soc.* **1995**, *117*, 11813. (d) Yam, V. W. W. *Chem. Commun.* **2001**, 789. (e) Dyer, J.; Grills, D. C.; Matousek, P.; Parker, A. W.; Towrie, M.; Weinstein, J. A.; George, M. W. *Chem. Commun.* **2002**, 872. (f) Yam, V. W. W.; Ko, C. C.; Zhu, N. Y. *J. Am. Chem. Soc.* **2004**, *126*, 12734. (g) Reece, S. Y.; Nocera, D. G. *J. Am. Chem. Soc.* **2005**, *127*, 9448. (h) Pomestchenko, I. E.; Polyansky, D. E.; Castellano, F. N. *Inorg. Chem.* **2005**, *44*, 3412. (i) Dirksen, A.; Kleverlaan, C. J.; Reek, J. N. H.; De Cola, L. *J. Phys. Chem. A* **2005**, *109*, 5248. (j) Gabriellson, A.; Hartl, F.; Zhang, H.; Smith, J. R. L.; Towrie, M.; Vlček, A.; Perutz, R. N. *J. Am. Chem. Soc.* **2006**, *128*, 4253. (k) Vlček, A.; Busby, M. *Coord. Chem. Rev.* **2006**, *250*, 1755. (l) McNally, A.; Forster, R. J.; Russell, N. R.; Keyes, T. E. *Dalton Trans.* **2006**, 1729. (m) Kirgan, R.; Simpson, M.; Moore, C.; Day, J.; Bui, L.; Tanner, C.; Rillema, D. P. *Inorg. Chem.* **2007**, *46*, 6464. (n) Casanova, M.; Zangrando, E.; Iengo, E.; Alessio, E.; Indelli, M. T.; Scandola, F.; Orlandi, M. *Inorg. Chem.* **2008**, *47*, 10407. (o) Shih, C.; Museth, A. K.; Abrahamsson, M.; Blanco-Rodríguez, A. M.; Di Bilio, A. J.; Sudhamsu, J.; Crane, B. R.; Ronayne, K. L.; Towrie, M.; Vlček, A.; Richards, J. H.; Winkler, J. R.; Gray, H. B. *Science* **2008**, *320*, 1760. (p) Probst, B.; Rodenberg, A.; Guttentag, M.; Hamm, P.; Alberto, R. *Inorg. Chem.* **2010**, *49*, 6453. (q) Takeda, H.; Koike, K.; Morimoto, T.; Inumaru, H.; Ishitani, O. Photochemistry and photocatalysis of rhenium(I) diimine complexes. In *Advances in Inorganic Chemistry, Vol 63: Inorganic Photochemistry*; VanEldik, R., Stochel, G., Eds.; Elsevier Academic Press Inc: San Diego, CA, 2011; Vol. 63, pp 137. (r) Stewart, D. J.; Brennaman, M. K.; Bettis, S. E.; Wang, L.; Binstead, R. A.; Papanikolas, J. M.; Meyer, T. J. *J. Phys. Chem. Lett.* **2011**, *2*, 1844. (s) Guo, D.; Knight, T. E.; McCusker, J. K. *Science* **2011**, *334*, 1684. (t) Kumar, B.; Llorente, M.; Froehlich, J.; Dang, T.; Sathrum, A.; Kubiak, C. P. *Annu. Rev. Phys. Chem.* **2012**, *63*, 541. (u) Windle, C. D.; Campian, M. V.; Duhme-Klair, A. K.; Gibson, E. A.; Perutz, R. N.; Schneider, J. *Chem. Commun.* **2012**, *48*, 8189. (v) Ordronneau, L.; Nitadori, H.; Ledoux, L.; Singh, A.; Williams, J. A. G.; Akita, M.; Guerschais, V.; Le Bozec, H. *Inorg. Chem.* **2012**, *51*, 5627. (w) Gatti, T.; Cavigli, P.; Zangrando, E.; Iengo,

E.; Chiorboli, C.; Indelli, M. T. *Inorg. Chem.* **2013**, *52*, 3190. (x) Dietrich, J.; Thorenz, U.; Förster, C.; Heinze, K. *Inorg. Chem.* **2013**, *52*, 1248. (y) Yue, Y. K.; Grusenmeyer, T.; Ma, Z.; Zhang, P.; Pham, T. T.; Mague, J. T.; Donahue, J. P.; Schmehl, R. H.; Beratan, D. N.; Rubtsov, I. V. *J. Phys. Chem. B* **2013**, *117*, 15903. (z) Larsen, C. B.; van der Salm, H.; Clark, C. A.; Elliott, A. B. S.; Fraser, M. G.; Horvath, R.; Lucas, N. T.; Sun, X. Z.; George, M. W.; Gordon, K. C. *Inorg. Chem.* **2014**, *53*, 1339.

(11) (a) Meylemans, H. A.; Hewitt, J. T.; Abdelhaq, M.; Vallett, P. J.; Damrauer, N. H. *J. Am. Chem. Soc.* **2010**, *132*, 11464. (b) Hanss, D.; Walther, M. E.; Wenger, O. S. *Coord. Chem. Rev.* **2010**, *254*, 2584. (c) Hanss, D.; Wenger, O. S. *Inorg. Chem.* **2008**, *47*, 9081. (d) Hanss, D.; Wenger, O. S. *Inorg. Chem.* **2009**, *48*, 671.

(12) Bozic-Weber, B.; Brauchli, S. Y.; Constable, E. C.; Furer, S. O.; Housecroft, C. E.; Wright, I. A. *Phys. Chem. Chem. Phys.* **2013**, *15*, 4500.

(13) (a) Sullivan, B. P.; Meyer, T. J. *J. Chem. Soc., Chem. Commun.* **1984**, 1244. (b) Smieja, J. M.; Kubiak, C. P. *Inorg. Chem.* **2010**, *49*, 9283.

(14) Hensel, V.; Schlüter, A. D. *Liebigs Ann.* **1997**, 303.

(15) (a) Brotschi, C.; Mathis, G.; Leumann, C. J. *Chem.—Eur. J.* **2005**, *11*, 1911. (b) Haino, T.; Araki, H.; Yamanaka, Y.; Fukazawa, Y. *Tetrahedron Lett.* **2001**, *42*, 3203.

(16) Hankache, J.; Hanss, D.; Wenger, O. S. *J. Phys. Chem. A* **2012**, *116*, 3347.

(17) Walther, M. E.; Grilj, J.; Hanss, D.; Vauthey, E.; Wenger, O. S. *Eur. J. Inorg. Chem.* **2010**, 4843.

(18) Noviadri, I.; Brown, K. N.; Fleming, D. S.; Gulyas, P. T.; Lay, P. A.; Masters, A. F.; Phillips, L. *J. Phys. Chem. B* **1999**, *103*, 6713.

(19) (a) Sacksteder, L.; Zipp, A. P.; Brown, E. A.; Streich, J.; Demas, J. N.; DeGraff, B. A. *Inorg. Chem.* **1990**, *29*, 4335. (b) Wallace, L.; Rillema, D. P. *Inorg. Chem.* **1993**, *32*, 3836. (c) Lever, A. B. P. *Inorg. Chem.* **1991**, *30*, 1980. (d) Bronner, C.; Wenger, O. S. *Inorg. Chem.* **2012**, *51*, 8275.

(20) (a) Sreenath, K.; Thomas, T. G.; Gopidas, K. R. *Org. Lett.* **2011**, *13*, 1134. (b) Lambert, C.; Nöll, G. *J. Am. Chem. Soc.* **1999**, *121*, 8434.

(21) Geiss, B.; Lambert, C. *Chem. Commun.* **2009**, 1670.

(22) (a) Kuss-Petermann, M.; Wolf, H.; Stalke, D.; Wenger, O. S. *J. Am. Chem. Soc.* **2012**, *134*, 12844. (b) Zalis, S.; Consani, C.; El Nahhas, A.; Cannizzo, A.; Chergui, M.; Hartl, F.; Vlček, A. *Inorg. Chim. Acta* **2011**, *374*, 578.

(23) (a) Katz, N. E.; Mecklenburg, S. L.; Meyer, T. J. *Inorg. Chem.* **1995**, *34*, 1282. (b) Lewis, J. D.; Bussotti, L.; Foggi, P.; Perutz, R. N.; Moore, J. N. *J. Phys. Chem. A* **2002**, *106*, 12202. (c) Chen, P. Y.; Westmoreland, T. D.; Danielson, E.; Schanze, K. S.; Anthon, D.; Neveux, P. E.; Meyer, T. J. *Inorg. Chem.* **1987**, *26*, 1116. (d) Bates, W. D.; Chen, P. Y.; Dattelbaum, D. M.; Jones, W. E.; Meyer, T. J. *J. Phys. Chem. A* **1999**, *103*, 5227. (e) Lopez, R.; Leiva, A. M.; Zuloaga, F.; Loeb, B.; Norambuena, E.; Omberg, K. M.; Schoonover, J. R.; Striplin, D.; Devenney, M.; Meyer, T. J. *Inorg. Chem.* **1999**, *38*, 2924.

(24) Pollnau, M.; Gamelin, D. R.; Lüthi, S. R.; Güdel, H. U.; Hehlen, M. P. *Phys. Rev. B* **2000**, *61*, 3337.

(25) Flamigni, L.; Baranoff, E.; Collin, J.-P.; Sauvage, J.-P.; Ventura, B. *ChemPhysChem* **2007**, *8*, 1943.

(26) (a) Gamelin, D. R.; Güdel, H. U. *Transition Metal and Rare Earth Compounds: Excited States, Transitions, Interactions* **2001**, *214*, 1. (b) Wenger, O. S.; Salley, G. M.; Valiente, R.; Güdel, H. U. *Phys. Rev. B* **2002**, *65*, 212108.

(27) Wightman, R. M.; Cockrell, J. R.; Murray, R. W.; Burnett, J. N.; Jones, S. B. *J. Am. Chem. Soc.* **1976**, *98*, 2562.

(28) Hankache, J.; Wenger, O. S. *Chem.—Eur. J.* **2012**, *18*, 6443.

(29) (a) Eckert, F.; Leitner, I.; Kaljurand, I.; Kütt, A.; Klamt, A.; Diedenhofen, M. *J. Comput. Chem.* **2009**, *30*, 799. (b) Kütt, A.; Leitner, I.; Kaljurand, I.; Soovali, L.; Vlasov, V. M.; Yagupolskii, L. M.; Koppel, I. A. *J. Org. Chem.* **2006**, *71*, 2829.

(30) Yago, T.; Gohdo, M.; Wakasa, M. *J. Phys. Chem. B* **2010**, *114*, 2476.

- (31) (a) Renger, G.; Renger, T. *Photosynth. Res.* **2008**, *98*, 53.
(b) Sinnecker, S.; Reijerse, E.; Neese, F.; Lubitz, W. *J. Am. Chem. Soc.* **2004**, *126*, 3280.
- (32) Pierri, A. E.; Pallaoro, A.; Wu, G.; Ford, P. C. *J. Am. Chem. Soc.* **2012**, *134*, 18197.
- (33) Hammarström, L.; Sun, L. C.; Åkermark, B.; Styring, S. *Spectrochim. Acta, Part A* **2001**, *57*, 2145.
- (34) (a) Meisel, D.; Matheson, M. S.; Mulac, W. A.; Rabani, J. *J. Phys. Chem.* **1977**, *81*, 1449. (b) Goez, M.; von Ramin-Marro, D.; Musa, M. H. O.; Schiewek, M. *J. Phys. Chem. A* **2004**, *108*, 1090.
- (35) Hankache, J.; Niemi, M.; Lemmetyinen, H.; Wenger, O. S. *J. Phys. Chem. A* **2012**, *116*, 8159.
- (36) (a) Wenger, O. S. *Acc. Chem. Res.* **2013**, *46*, 1517.
(b) Melomedov, J.; Ochsmann, J. R.; Meister, M.; Laquai, F.; Heinze, K. *Eur. J. Inorg. Chem.* **2014**, *2014*, 1984.
- (37) Bruker AXS Inc.: Madison, WI, 2006.
- (38) Palatinus, L.; Chapuis, G. *J. Appl. Crystallogr.* **2007**, *40*, 786.
- (39) Betteridge, P. W.; Carruthers, J. R.; Cooper, R. I.; Prout, K.; Watkin, D. J. *J. Appl. Crystallogr.* **2003**, *36*, 1487.
- (40) Carruthers, J. R.; Watkin, D. J. *Acta Crystallogr., Sect A* **1979**, *35*, 698.
- (41) Macrae, C. F.; Bruno, I. J.; Chisholm, J. A.; Edgington, P. R.; McCabe, P.; Pidcock, E.; Rodriguez-Monge, L.; Taylor, R.; van de Streek, J.; Wood, P. A. *J. Appl. Crystallogr.* **2008**, *41*, 466.